

ESD-TDR-64-332

# ESD RECORD COPY

RETURN TO  
SCIENTIFIC & TECHNICAL INFORMATION DIVISION  
(ESTI), BUILDING 1211

COPY NR. \_\_\_\_\_ OF \_\_\_\_\_ COPIES

## ESTI PROCESSED

ODC TAB     PROJ OFFICER

ACCESSION MASTER FILE

\_\_\_\_\_

DATE \_\_\_\_\_

ESTI CONTROL NR **AL 43006**

CY NR 1 OF 1 CY#

# Technical Report

# 356

## Limitations of Oxide-Cathode High Current Density Operation

H. A. Pike

22 May 1964

Prepared for the Advanced Research Projects Agency  
under Electronic Systems Division Contract AF 19(628)-500 by

# Lincoln Laboratory

MASSACHUSETTS INSTITUTE OF TECHNOLOGY

Lexington, Massachusetts



AD 604890





MASSACHUSETTS INSTITUTE OF TECHNOLOGY

LINCOLN LABORATORY

LIMITATIONS OF OXIDE-CATHODE  
HIGH CURRENT DENSITY OPERATION

*H. A. PIKE*

*Group 43*

TECHNICAL REPORT 356

22 MAY 1964

LEXINGTON

MASSACHUSETTS

## ABSTRACT

Micrasecond pulsed current from a good oxide cathode at normal operating temperatures is often limited by sparking rather than by saturation of cathode emission. Measurements have been made of the current at which sparking occurs for pulse lengths between 0.5 and 500  $\mu$ sec. Also, the fast time response of photomultiplier tubes sensitive in the near infrared has allowed the measurement of temperature transients on the cathode surface during and after the pulse. It was found that the current which caused a fixed cathode surface temperature rise was dependent upon pulse length, as was the sparking current. The supposition is made that, for short pulses, sparking is associated with the thermal dissociation of the cathode coating surface due to joule heat generated by the passage of current through the high resistance layer at the surface of the coating. Increasing the anode temperature decreased both the cathode work function and coating resistance. Using this technique, current density in excess of  $200 \text{ amp/cm}^2$  was drawn without sparking.

Accepted for the Air Force  
Franklin C. Hudson, Deputy Chief  
Air Force Lincoln Laboratory Office

## TABLE OF CONTENTS

Abstract	iii
I. Introduction	1
II. Experimental Vehicles	3
III. Sparking Experiments	3
IV. Some Effects of Anode Temperature	7
V. Measurements of Temperature Transients on the Cathode Surface	9
VI. Interpretations	10
A. Cathode- and Anode-Initiated Sparking	10
B. Mechanism of Temperature Rise During Pulse	11
VII. Summary	12
Appendix – Cathode Processing	15
I. Conversion Techniques	15
II. ASTM Diode Slow-Vacuum Conversion	15
III. ASTM Diode Fast-Vacuum Conversion	16
IV. Coomes Diode Conversion	16

# LIMITATIONS OF OXIDE-CATHODE HIGH CURRENT DENSITY OPERATION

## I. INTRODUCTION

In modern vacuum electronic devices, the limit of high power, as well as high frequency in some situations, is often imposed by the amount of current density that may be drawn from the cathode. Pulsed oxide cathodes in high-power tubes are usually operated in the range between 1 and 10 amp/cm<sup>2</sup> although current densities of over 100 amp/cm<sup>2</sup> have been achieved by Coomes, *et al.*,<sup>1,2</sup> and Pomerantz.<sup>3</sup> The work described in this report was undertaken to study the factors which limit pulsed emission from such cathodes and which cause the large gap between practical design values for cathode current density and the values which have been reached in carefully processed laboratory cathodes.

There are two ways in which the cathode current density may be limited. The most common is saturation of cathode emission. When a current greater than the zero-field-emission current is drawn, the cathode changes from space-charge-limited to temperature-limited operation. Saturation in oxide cathodes is seldom sharp because there are anomalous Schottky effects and voltage drops within the oxide coating. However, a region is usually reached in which an increase in the anode-to-cathode voltage causes only a small increase in cathode current. Reduction of this emission capability is often observed during the pulse<sup>4-9</sup> and is usually attributed to either return of gas from the anode or diffusion of activating agents away from the cathode surface. Nergaard's mobile donor hypothesis describes this decay with a semiconductor model in which the donors electrolyze away from the surface because of the electric field present in the coating during the drawing of current.

The other limitation of pulsed current is sparking within the tube. The work of Coomes, Buck, Fineman, and Eisenstein<sup>1,2</sup> at the Radiation Laboratory, M.I.T., established that the oxide cathode was capable of pulsed emission greater than 100 amp/cm<sup>2</sup> (Refs. 1, 2). Using high purity nickel bases, they were able to achieve space-charge-limited, 1- $\mu$ sec pulses of as much as 130 amp/cm<sup>2</sup> before sparking occurred. The influence of the base metal impurities on sparking was shown later by Eisenstein.<sup>10</sup> He demonstrated that the barium orthosilicate layer which forms between the oxide coating and a Si-Ni alloy base reduces the sparking current from more than 100 to less than 10 amp/cm<sup>2</sup>. His data indicated that sparking was due to joule heating in the barium orthosilicate interface.

Ramsey,<sup>11</sup> Pomerantz,<sup>3</sup> Danforth and Goldwater<sup>12</sup> of the Bartol Research Foundation have also studied high-space-charge-limited sparking currents. Pomerantz found that drawing a steady DC current from the cathode allowed the sparking current to increase from 45 amp/cm<sup>2</sup> (no DC component) to 150 amp/cm<sup>2</sup> (1 amp/cm<sup>2</sup> DC component), which was ascribed to a reduction of



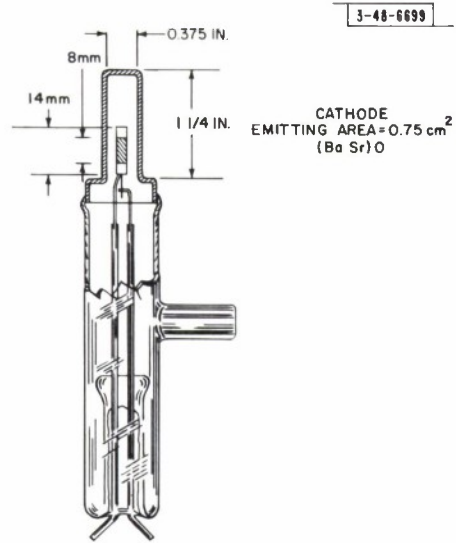


Fig. 1. Coomes diode.

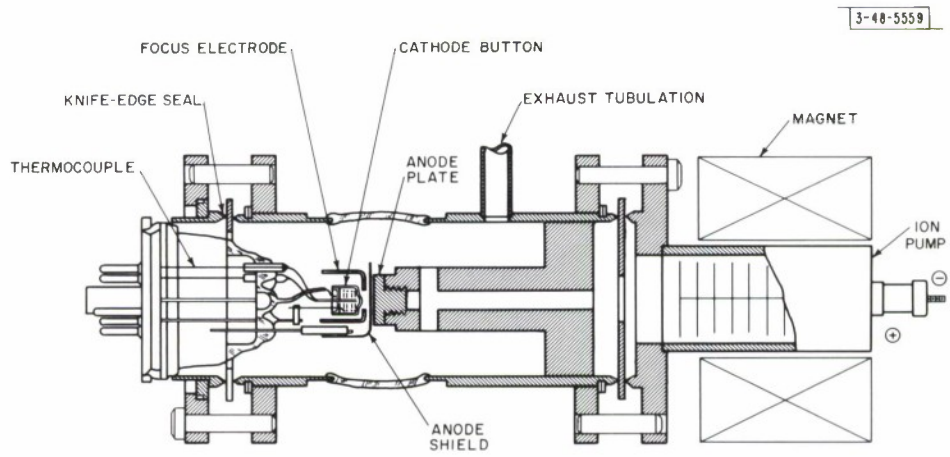


Fig. 2. Sperry ultraclean diode with ion-getter pump.

coating resistance with increased DC component, an effect studied by Danforth and Goldwater. According to their theory, this reduction allowed a greater current to be drawn, before the field necessary for dielectric breakdown occurred. Ramsey noted that the pulse length between 10 and 100  $\mu$ sec, for which sparking occurred, was proportional to  $(1/I_a V_a)^{1/2}$ , where  $I_a V_a$  is the anode power. Since this relationship is the same as the time required for the anode surface to reach a fixed temperature, he associated the sparking with a release of gas from the anode when bombardment had heated it to a critical temperature  $T_{AC}$ .

## II. EXPERIMENTAL VEHICLES

Three types of tubes were used: the ASTM (The American Society for Testing Materials) standard cylindrical diode,\* a cylindrical diode of the type used by Coomes (Fig. 1), and the Sperry ultraclean diode<sup>13</sup> (Fig. 2). All the cathodes had high-purity passive bases to avoid the formation of an interface compound. Processing schedules are given in the Appendix.

The ASTM diodes were made of 499 nickel with a sprayed cathode coating of  $(\text{BaSr})\text{CO}_3$ . Temperature measurements were estimated from optical pyrometer readings taken on the tube's cathode sleeve, where it extended beyond the anode cylinder, and from readings taken from a similar tube with a small hole in the anode. Since the cathode coating was hidden by the anode cylinder, it was impossible to measure temperature transients during the pulse in this tube. A standard Bayard-Alpert gauge with the Nottingham modification<sup>14</sup> was attached to the envelope to monitor the pressure within the tube.

The Coomes diode first used had a 499 nickel base and a sprayed coating of  $(\text{BaSr})\text{CO}_3$ . The kovar anode was part of the tube envelope, which facilitated control of the anode temperature. The entire cathode coating was visible allowing both average- and short-time temperature measurements. The tubes which were used later also had a Pt - Pt + 10% Rh thermocouple on the cathode.

The Sperry ultraclean diode, built and converted by the Sperry Gyroscope Company, had an attached ion pump and a Pt - Pt + 10% Rh thermocouple on the cathode. The cathode base, either 499 nickel or platinum, had a sprayed  $(\text{BaSrCa})\text{CO}_3$  coating. The metal flanges and exhaust tubulation allowed final sealing operations without contamination from glass decomposition products.

## III. SPARKING EXPERIMENTS

The current and voltage at which sparking occurred ( $I_s$  and  $V_s$ ) were measured for pulse lengths from 0.5 to 500  $\mu$ sec and for the normal range of operating temperatures. The pulse-recurrence frequency was, in general, set low enough (below 20 cps) so that changing it had no effect on sparking parameters. Then the voltage was increased until sparking occurred on several consecutive pulses after which the voltage was removed and the pulse length adjusted to a new value. It was usually possible, after completing a set of measurements, to duplicate the values from the first set of measurements to within 15 percent. Occasionally, sparking would either improve or degrade tube performance considerably, and the measurements would have to be repeated. It was often observed that when sparking caused the saturated emission to improve, the current and voltage at which sparking occurred would also increase.

---

\* ASTM designation: F270-56 (adapted 1956).



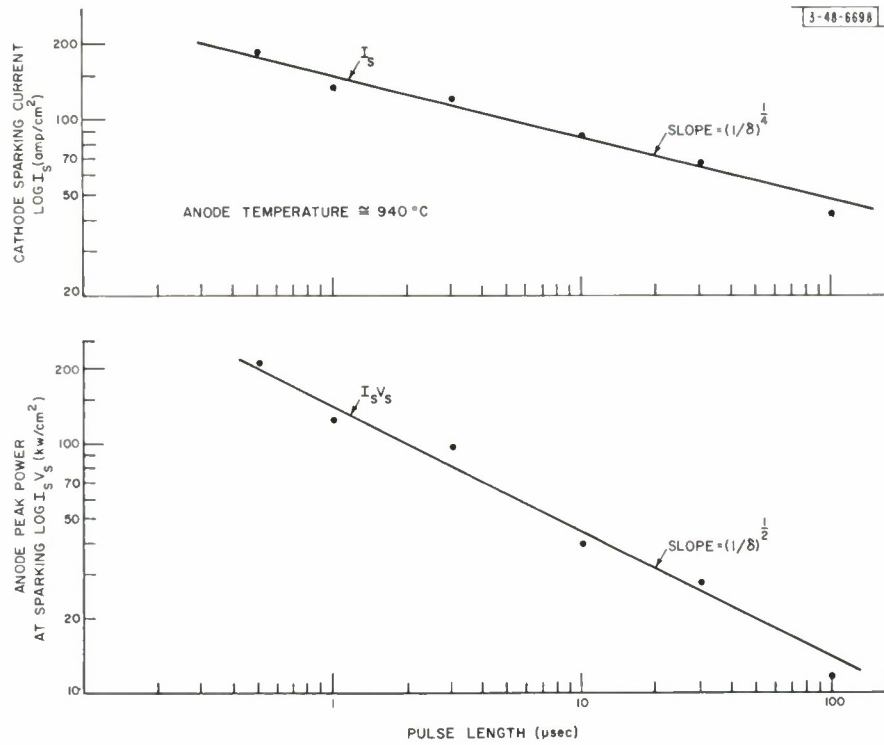


Fig. 3. Sparking current and power for ASTM diode NS-5.

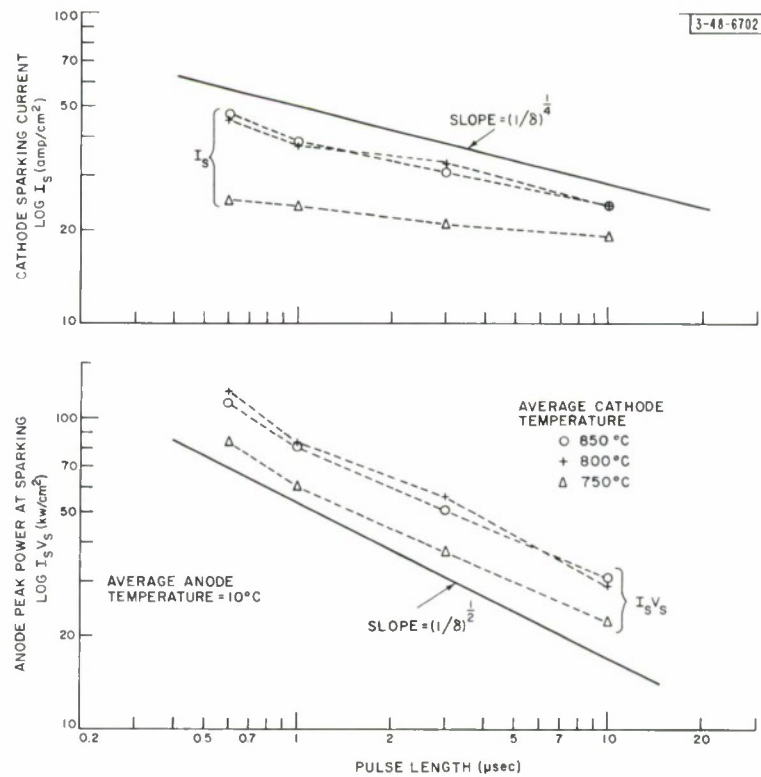


Fig. 4. Sparking current and power for Coomes diode 2.

Within experimental uncertainty, all the tubes showed the same relationship of sparking current  $I_s$ , and sparking voltage  $V_s$ , to the pulse length  $\delta$ . The results are shown in Figs. 3 to 5. If the anode power at sparking is plotted against the pulse length  $\delta$ , the same variation that Ramsey observed is found to apply, i.e.,  $I_s V_s$  is proportional to  $(1/\delta)^{1/2}$  where  $\delta$  is the pulse length. However, if the sparking current is plotted against the pulse length, the relation  $I_s \sim (1/\delta)^{1/4}$  also fits most of the points. If the current is space-charge limited, as it usually was, the relation  $I_s V_s = (a/\delta)^{1/2}$  requires that  $I_s = (b/\delta)^{3/10}$ . The uncertainties involved in these measurements made it difficult to distinguish between a slope of 0.25 and 0.30. If the current has begun to saturate, the slope would be even less than 0.30. Decreasing the cathode temperature decreases the current at which sparking occurs, although the data are not consistent enough to yield an activation energy for the change.

The effect of the anode temperature on the 1/2- $\mu$ sec pulse sparking is shown in Figs. 6 and 7, where the sparking points are indicated by crosses. Increasing the anode temperature of the Coomes diode not only increases the sparking point but also the saturated emission. This effect is discussed further in Sec. IV. The data shown in Fig. 7 are difficult to interpret since the ASTM diode anode temperature can only be controlled by increasing the pulse-recurrence frequency which also increases the cathode temperature. However, when the cathode temperature

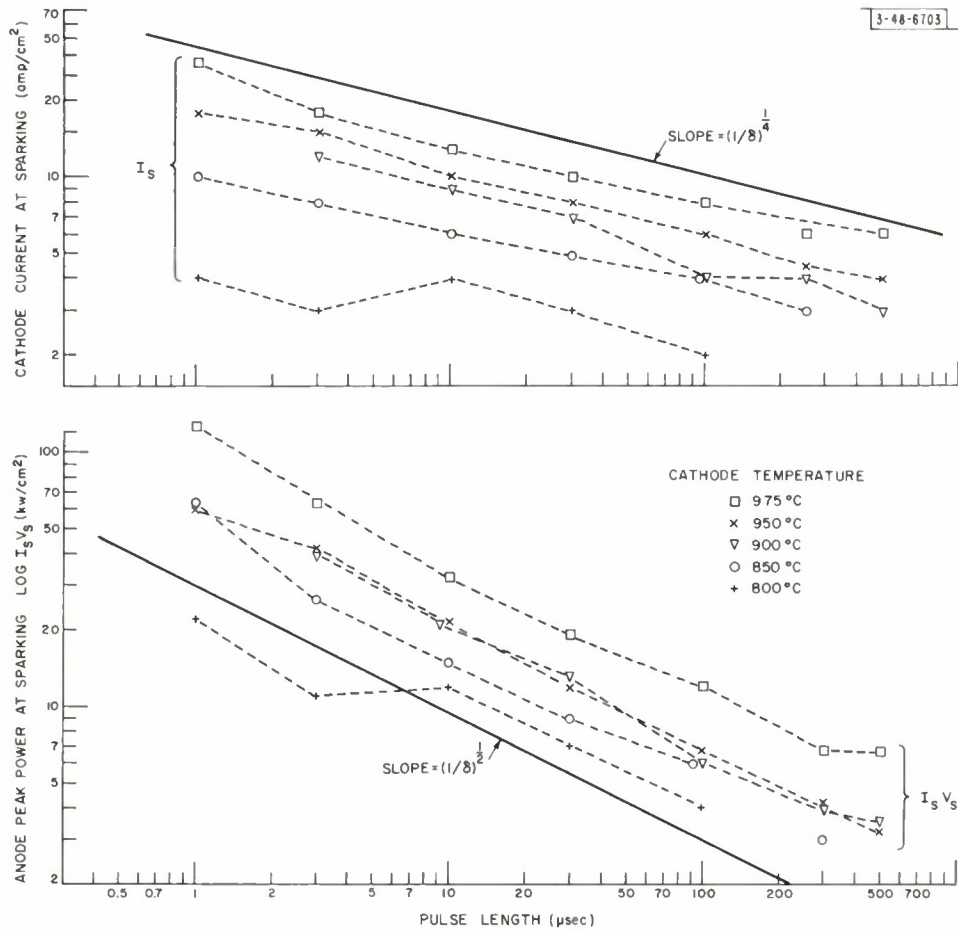


Fig. 5. Sparking current and power for Sperry ultraclean diode 589.

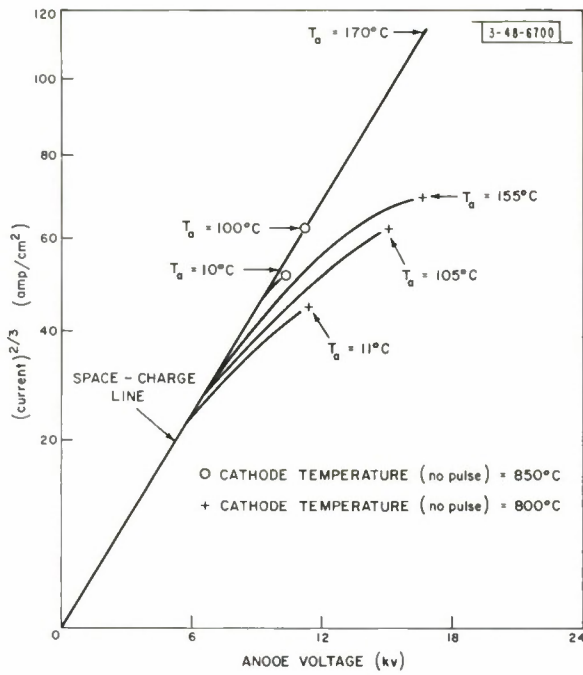
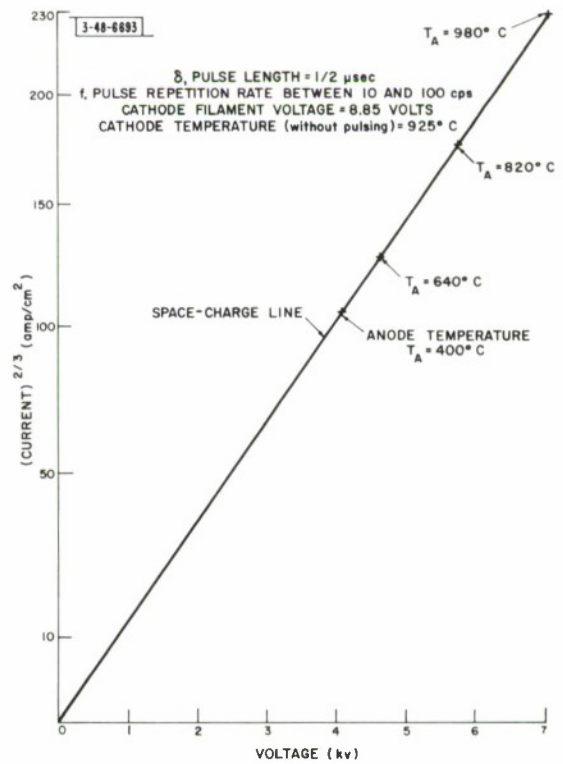


Fig. 6. Effect of anode temperature on sparking, Coomes diode 2.

Fig. 7. Effect of anode temperature on sparking, ASTM diode NS-1.



was raised the same amount by increasing the heater power, but keeping the prf constant, only an 8 percent increase in the sparking current was observed.

It was thought that increasing the anode temperature might remove enough foreign material from the anode to leave it relatively clean and make sparking more difficult. However, retarding-field measurements made later on the Coomes diodes indicated that raising the anode temperature from 10° to 200°C did not remove sufficient foreign material from the anode to affect its work function, whose value, 2.0 ev, was about half that expected for clean kovar.

#### IV. SOME EFFECTS OF ANODE TEMPERATURE

The cathode coating resistance can be measured by equating the average power delivered to the coating by joule heating with the average temperature rise  $\Delta T_{av}$  of the cathode times a constant  $k$ (watts/°C) determined from the slope of the temperature vs heater power curve,

$$R \cdot I^2 \cdot \delta \cdot f = k\Delta T \quad ,$$

where  $f$  is the pulse-recurrence frequency. Measurements made using this method have been reported by Coomes.<sup>2</sup> Results similar to those he reported were achieved in measurements of a Coomes diode with the anode at 10°C (Fig. 8). However, when the anode was heated to 150°C, the average temperature rise under the same conditions was so small that it could not be detected.

A similar decrease in joule heating was observed in the ASTM diodes as the anode became hot (Fig. 9). Figure 10 shows how the effective work function, pressure, and anode temperature vary at the same time. It appears that heating the anode, whether externally, as in the Coomes diode, or by electron bombardment, as in the ASTM diode, has two effects on the cathode: (1) a decrease in coating resistance (Figs. 9 and 10) and (2) a decrease in effective work function (Figs. 6 and 10). In the ASTM diodes, these two effects could be caused by the high average current required to heat the anode, which might create free barium or, more generally, donor centers in the cathode coating both by electrolysis and by thermal dissociation, as in the well-known current-activating techniques. However, in the Coomes diodes, the two effects could be

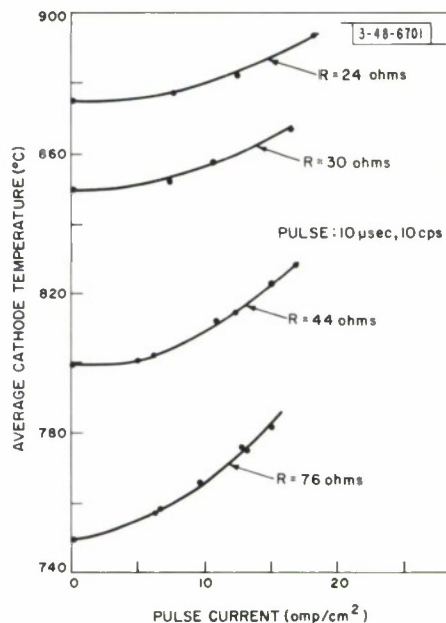


Fig. 8. Joule heating in Coomes diode 2.



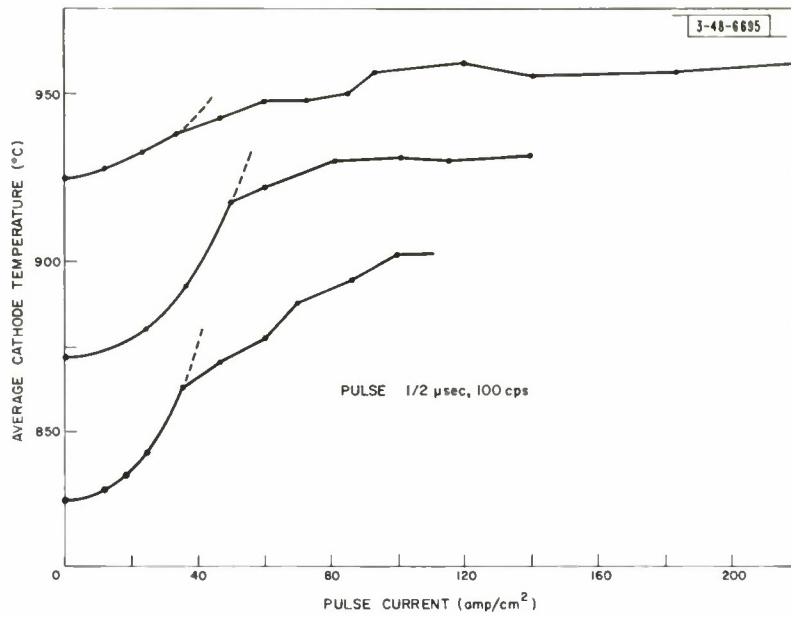


Fig. 9. Joule heating in ASTM diode NS-5.

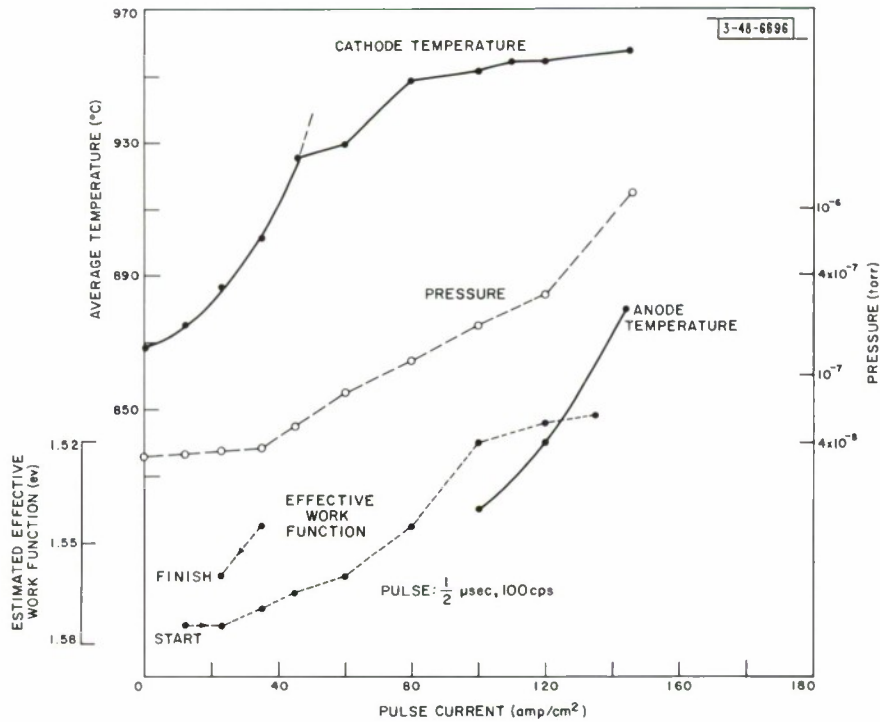


Fig. 10. Some effects of high pulse current in ASTM diode NS-5.

caused by the anode temperature alone through return to the cathode of free barium evaporated into the anode.

## V. MEASUREMENTS OF TEMPERATURE TRANSIENTS ON THE CATHODE SURFACE

Rapid temperature changes on cathode surfaces have been measured before; however, in one case<sup>15,16</sup> time and current dependences were not reported, and in the other<sup>17</sup> the cathode was operated in a gas discharge, the temperature rise was apparently due to back bombardment by ions, and hence the results are not applicable to vacuum cathodes. In both of these cases, the intensity of the thermal radiation was measured with a photosensitive device capable of responding in times short compared with the pulse length.

In the measurements reported here, a 7102 photomultiplier tube was used in conjunction with a filter, which cut out radiation of wavelengths less than  $7700 \text{ \AA}$ , and an optical system whose small acceptance angle ( $\frac{1}{2}^\circ$ ) allowed observation of the Coomes diode cathode coating to the exclusion of the surrounding surfaces. The instrument was calibrated against the thermocouple attached to the cathode. The calibration curve followed that computed from the Planck radiation law and the characteristics of the photomultiplier. The signal across the anode-to-ground resistance was viewed with an oscilloscope, and the resistance varied until a response time of about  $1 \mu\text{sec}$  was achieved. Similar apparatus was used by E. Silverman of this Laboratory in measuring pulse temperatures of bombarded metallic surfaces.<sup>18</sup> No temperature change was discernible on the nickel cathode sleeve or the anode. Since the temperature distribution over the cathode surface during the pulse was not measured, the temperatures shown in Figs. 11 to 13 were measured on the assumption that the pulse-temperature rise is uniform over the cathode area viewed by the optical system. If, as may be the case, the temperature rise is experienced only by small areas on the coating, the so-called "hot spots," then the temperature of these areas would be greater than that derived from the above assumption.

The increase of the cathode surface temperature during the pulse is expressed in Fig. 11 as the normalized temperature rise  $T - T_0 / T_\delta - T_0$  vs the normalized time  $t - t_0 / t_\delta - t_0$  for pulse lengths from 10 to 100  $\mu\text{sec}$  ( $T_0$  and  $t_0$  are the temperature and time at the beginning of the pulse;

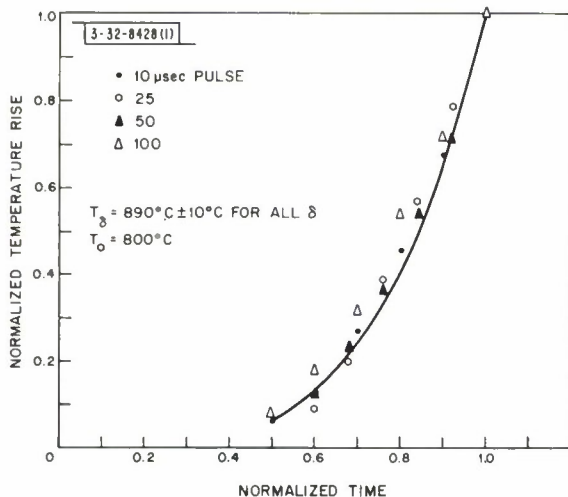


Fig. 11. Rise of cathode surface temperature during a pulse.

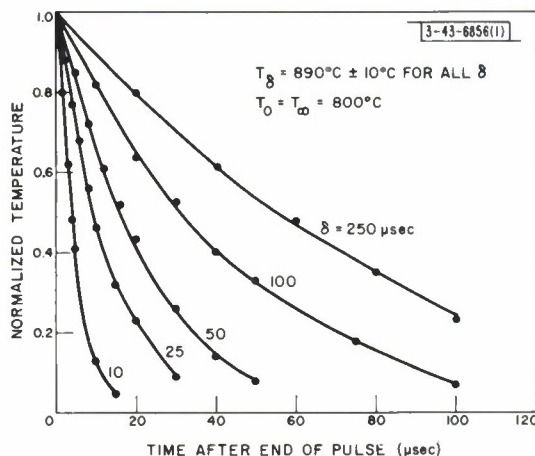


Fig. 12. Relaxation of cathode surface temperature after a pulse.

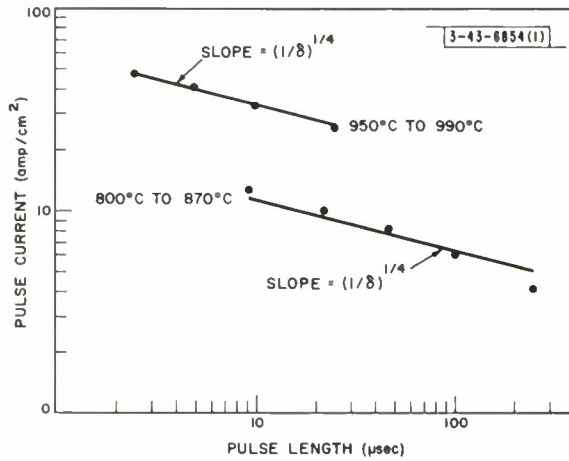


Fig. 13. Current and pulse length relationship for a fixed cathode surface temperature rise.

$T_\delta$  and  $t_\delta$  are the temperature and time at the end of the pulse). Contrary to expectations, the surface temperature increases more rapidly than linearly with time, which seemed to occur for all pulse lengths studied. In Fig. 12, the normalized temperature  $T - T_\infty / T_\delta - T_\infty$  is plotted against the time after the end of the pulse. It is apparent that the time required for the relaxation of the surface temperature is proportional to the length of the heating pulse, which has important consequences when the mechanism of the temperature transients is considered.

In Figs. 11 and 12, the current for each pulse length was adjusted so that the surface temperature at the end of the pulse would be approximately the same for all pulse lengths. This adjustment meant that the current for longer pulses was decreased. The exact relation is shown in Fig. 13. The current required for a fixed temperature rise during the pulse – from  $800^\circ$  to  $870^\circ\text{C}$  in one case, from  $950^\circ$  to  $990^\circ\text{C}$  in the other – is plotted vs the pulse length. In both cases, the relation  $I \sim (1/\delta)^{1/4}$  holds as it did for the sparking current.

## VI. INTERPRETATIONS

### A. Cathode- and Anode-Initiated Sparking

For the pulse lengths and beam voltages used, the surface heating approximation applies to the anode.<sup>19</sup> This approximation gives the well-known result, a rise in surface temperature of the anode proportional to the square root of the pulse length times the incident power, that is,  $\Delta T_A = CI_A V_A \sqrt{\delta}$ . If the release of sufficient gas from the anode to initiate sparking is associated with a critical anode temperature  $T_{AC}$ , then one can write  $I_S V_S = (T_{AC} - T_{A0}) / c\sqrt{\delta}$  (Ramsey called this sparking anode-initiated sparking), which also corresponds to the dependence of sparking current and voltage found in our experiments, assuming that  $T_{AC} - T_{A0}$  remains constant.

On the other hand, the measurements of the cathode surface temperature indicate that the current required for a fixed cathode surface temperature rise is inversely proportional to the fourth root of the pulse length. If sparking is associated with the release of gas from the cathode surface by thermal dissociation of the surface coating which occurs at a critical temperature, then for a fixed initial cathode temperature  $I_S = d(1/\delta)^{1/4}$ , which also fits the data reported above. It is not possible, therefore, to distinguish between anode- and cathode-initiated sparking phenomena on the basis of the dependence of the sparking current and voltage on pulse length alone.

For 0.5- $\mu$ sec pulses, heating the anode increased the sparking current and also reduced the cathode coating resistance. The increased short pulse sparking current with increased anode temperature can be understood in terms of the cathode-initiated sparking model since the coating resistance is reduced. Moreover, joule heating could cause the same temperature rise because the current can be greater when the coating resistance is reduced.

Interpretation of the evidence in favor of anode-initiated sparking is more difficult. It seems implausible that heating the anode might remove enough gas to increase the term  $T_{AC} - T_{A0}$ , even though  $T_{A0}$  increased, because the anode work function does not change when the anode is heated. Thus, it seems that, for short pulses, sparking is caused by thermal dissociation of the cathode coating due to joule heating caused by the pulse current.

There is evidence that anode phenomena may become more important in sparking at longer pulse lengths. Sparking current data for hot and cold anodes, taken late in the life of one Coomes diode, showed a crossover at about 50  $\mu$ sec. For pulses shorter than 50  $\mu$ sec, heating improved the sparking characteristic; for longer pulses, it decreased the sparking current.

### B. Mechanism of Temperature Rise During Pulse

There is some disagreement about the mechanism of conduction in the oxide cathode. Hannay, MacNair, and White<sup>20</sup> describe a modern semiconductor model in which conduction is by electrons. Loosjes and Vink<sup>21</sup> contend that conduction is by electrons in the pores of the oxide matrix. The following discussion will be based on the semiconductor model, but would be little altered by assuming pore conduction.

Theoretical calculations of temperature transients have been made by Campbell<sup>9</sup> on the assumption that joule heating occurred uniformly throughout the coating and that the cathode base temperature did not change during the pulse. In that case, there exists a time constant for the relaxation of the surface temperature after the pulse which is independent of the pulse length. However, Fig. 12 shows that the relaxation time is proportional to the length of the heating pulse, which is consistent with a model in which heating occurs at the cathode surface and heat diffuses in toward the cathode base. For a short pulse, the temperature gradient near the surface is quite large, and the surface temperature decays rapidly after the pulse is turned off. For a longer pulse, more heat diffuses into the coating interior, and the temperature gradient at the surface is less; thus temperature decay is less rapid. These conclusions are supported by a solution to the heat equation for oxide-cathode surface heating given by Clogston.<sup>22</sup>

A large difference between the joule heating in the body of the coating and near the surface is not surprising, since other investigators have found that (1) preferential evaporation of BaO from a (BaSr)O coating yields a surface composed largely of SrO (Ref. 23); (2) a large voltage drop occurs at the surface of the coating when pulse currents are drawn.<sup>24</sup> Still other investigators have also found evidence for the existence of a high-resistance layer near the cathode coating surface.<sup>16,25</sup> If the power input to the cathode coating surface were constant during the pulse, one would expect the temperature to rise as the square root of time for the range of pulse lengths considered, as in anode heating. However, Fig. 11 showed that the temperature rise is faster than linear with time. (The heat loss due to evaporated electrons, equal to the current times the electron affinity,<sup>9</sup> is small compared to that necessary to cause the observed temperature rises.) Therefore, the rapid increase in cathode surface temperature with time can only be explained by postulating a source of heat which increases during the pulse, i.e., the resistance of the coating surface must increase during the pulse.



Such an increase could be explained by Nergaard's mobile donor hypothesis,<sup>5</sup> mentioned earlier in connection with decay of thermionic emission, since the reduction in donor concentration would also increase the resistance of the surface region. An equation for the reduction of surface donor concentration during a steady current pulse is given by Frost<sup>6</sup> as

$$n_d(x, t) = n_{do} - 4 \frac{n_{do} I R_o q_o}{\pi^2 K T} \sum_{m=1}^{\infty} \frac{1}{(2m-1)^2} \left\{ 1 - \exp \left[ - \frac{\pi^2 (2m-1)^2 D t}{d^2} \right] \right\} \\ \times [\cos \pi (2m-1) \frac{x}{d}] \quad ,$$

where

- $n_d$  is the donor concentration,
- $n_{do}$  is the average donor concentration before the pulse,
- $x$  is the distance from the coating surface,
- $t$  is the time from the beginning of the pulse,
- $I$  is the current,
- $R_o$  is the initial resistance of the coating,
- $q_o$  is the initial average donor charge,
- $T$  is the temperature,
- $D$  is the donor diffusion constant,
- $d$  is the coating thickness.

When Frost's values for  $q_o$  and  $D$  and a typical experimental value for  $R_o$  were used, it was found that the decrease of surface donor concentration became significant for currents and pulse lengths of the magnitude shown in Fig. 13. The decrease in donor concentration was nearly constant for distances less than 1 micron away from the surface and was insignificant for distances greater than 10 microns. Since surface roughness of the coating is greater than 10 microns, it did not seem worthwhile to pursue the results of this equation which was based on a smooth surface model, beyond pointing out that significant redistribution of donors could be expected within the bounds of our experiments.

## VII. SUMMARY

Data have been presented which show that the relation between the current which causes a fixed cathode surface temperature rise and pulse length is the same as the relation between current at which sparking occurs and pulse length. Since increasing the anode temperature increased the sparking current, it is believed that the anode does not have a dominant role in microsecond sparking and that sparking is initiated by the thermal dissociation of cathode surface material. The behavior of the cathode surface temperature during and after the current pulse seems to indicate that the temperature increase is caused by joule heating of the cathode surface region whose resistance increases during the pulse as a result of field-enhanced migration of donors away from the surface.

It is believed that the large current densities achieved were possible because surface donor depletion was prevented by an excess concentration of donors in the cathode surface region. This excess was apparently caused by the presence of a hot anode which may have provided a means for the return of free barium to the cathode.

#### ACKNOWLEDGMENTS

I am indebted to Professor E. A. Coomes of the University of Notre Dame for his helpful discussions and for parts that were used in some of the tubes. I wish also to thank the many members of Lincoln Laboratory who helped in this investigation, in particular, F. T. Worrell, R. C. Butmon, G. L. Guernsey, and P. Youtz.

## APPENDIX CATHODE PROCESSING

### I. CONVERSION TECHNIQUES

Three types of conversion techniques were studied. The first, referred to as slow conversion, corresponds to the method generally used by high-power tube manufacturers. In this technique, the temperature of the cathode is increased at such a rate that the pressure in the tube does not exceed some previously selected limit such as  $10^{-5}$  torr. In the second type, fast conversion, the cathode temperature is raised abruptly in one or two steps to conversion temperature; the pressure usually exceeds  $10^{-3}$  torr for a short time until the cathode carbonate is converted to oxide and the gas is pumped away. In the third method, that of MacNair of Bell Telephone Laboratories, the cathodes are converted in an atmosphere of hydrogen which is evacuated after conversion. This method has the advantage that initial contamination of electrodes by the conversion products, which must be prevented by other means in vacuum, is prevented by the reducing atmosphere of hydrogen.

The initial results of ASTM diode conversion tests indicated that the hydrogen-converted cathodes were capable of two to three times the emission of the vacuum-converted cathodes. Later, when we had refined our vacuum-processing and activation techniques, we found that the vacuum-converted cathodes were superior. The results of the latest tests have shown that there was little difference between the slow- and fast-vacuum-converted tubes and that the vacuum-converted tubes were as a group capable of about three times the emission density available from hydrogen-converted cathodes. A review of our experiments and discussions with the Cathode Research Group at Bell Telephone Laboratories led us to believe that the range of conversion temperatures and times we investigated for hydrogen conversion was greater than the optimum. When we opened the tubes and inspected the cathode we discovered that the hydrogen-converted cathodes appeared to have sintered coatings with the nickel base visible between groups of sintered particles. It appears that a hydrogen-converted cathode is much easier to activate than a vacuum-converted cathode when care has not been taken to prevent contamination of nearby electrodes in the vacuum-processed tube.

The cathode-conversion chamber used for both ASTM and Coomes diodes was prepared as follows:

- (a) The diode was sealed onto the pumping system which was then evacuated and checked for leaks using a portable vacuum system with a helium-sensitive leak detector.
- (b) The chamber was baked for two hours at  $150^{\circ}\text{C}$ .
- (c) The valve to the high-vacuum system was then opened and the chamber baked at  $400^{\circ}$  to  $450^{\circ}\text{C}$  for 10 hours.

Since the data reported above did not include any hydrogen-converted diodes, only the vacuum conversion will be described.

### II. ASTM DIODE SLOW-VACUUM CONVERSION

When the high-temperature vacuum bake had been completed, the anode was heated to  $750^{\circ}\text{C}$  for one minute by RF induction heating. After the anode cooled, the cathode was heated in stages, keeping the pressure below  $10^{-5}$  torr until the filament voltage reached 3.5 volts. At this voltage,

the binder has usually been driven off. Then the anode temperature was raised to and held at 850°C. It was found that raising the anode temperature to this point any sooner in the processing would greatly increase the time required to drive off the binder and to convert the carbonate to oxide. The cathode voltage was then increased in steps to 7.5 volts (the cathode temperature was 850°C) keeping the tube pressure below  $10^{-5}$  torr. By this time, a sharp drop in pressure had usually occurred indicating that conversion had been completed. The filament voltage was then raised abruptly to 12 volts and held for 5 minutes after which the voltage was returned to 7.5 volts and the anode was allowed to cool.

### III. ASTM DIODE FAST-VACUUM CONVERSION

After the high-temperature bake the cathode-filament voltage was raised immediately to 7.5 volts and the anode temperature was simultaneously raised to 850°C. The system pressure would then rise to the  $10^{-2}$  torr range for about a minute and fall back below  $10^{-5}$  torr. When the pressure was below  $5 \times 10^{-7}$  torr, the filament voltage was increased to 12.0 volts for 5 minutes and then reduced to 7.5 volts, and the anode was allowed to cool.

### IV. COOMES DIODE CONVERSION

We used the technique described by Coomes, *et al.*<sup>1</sup> The very thorough appendix of their report is to be recommended to anyone interested in the details of vacuum tube construction, cleaning and processing. The section on conversion is quoted here.

"1. Binder removal: The cathode power is set at approximately 3 watts; the pressure should not go above  $5 \times 10^{-5}$  mm. This temperature is held for a few minutes and then the heater power is increased to about 3.5 watts. As the cathode is held at this temperature for a few minutes, it can be observed visually that during this procedure it changes in color from a light gray to a patchy white to a pure white. Experience indicates that the cathode must be put into this state if a sharp and complete conversion is desired.

"2. Conversion: After removal of the binder the cathode temperature is raised immediately in one step to between 850° – 900°C, and held at this temperature until conversion is complete. (During conversion the emissivity of the cathode decreases so that the heater voltage must be decreased correspondingly to maintain a constant temperature.) If conversion is proper the pressure at the end of breakdown should fall from  $10^{-3}$  mm to below  $10^{-6}$  mm in a few minutes or less. Experience has shown that a cathode whose pressure lingers at some value above  $10^{-6}$  mm after conversion is most generally poor for pulsc applications."

The Coomes diode was activated on the pump. A DC potential applied between cathode and anode was increased slowly until 25 ma/cm<sup>2</sup> was drawn. The ASTM diodes were activated both before and after they were sealed off from the pumping system. A DC potential was applied until 50 ma/cm<sup>2</sup> was drawn. This current density was generally drawn for several hours before the tube was sealed off. After sealoff the diodes were found to reach maximum pulsc emission only after 50 ma/cm<sup>2</sup> had been drawn for several days.



## REFERENCES

1. E. A. Coomes, J. G. Buck, A. S. Eisenstein, and A. Finemon, "Alkaline Earth Oxide Cathodes for Pulsed Tubes," Report 933, Radiation Laboratory, M. I. T. (30 March 1946).
2. E. A. Coomes, "The Pulsed Properties of Oxide Cathodes," J. Appl. Phys. 17, 647 (1946).
3. M. A. Pomerantz, "Magnetron Cathodes," Proc. IRE 34, 903 (1946).
4. R. L. Sproull, "An Investigation of Short-Time Thermionic Emission from Oxide-Coated Cathodes," Phys. Rev. 67, 166 (1945).
5. L. S. Nergoord, "Studies of the Oxide Cathode," RCA Rev. 13, 464 (1952).
6. H. B. Frost, "Transient Changes in Oxide Cathodes," DSc Thesis, Department of Electrical Engineering, M. I. T. (September 1954).
7. H. J. Krusemeyer and M. V. Pursley, "Donor Changes in Oxide-Coated Cathodes," J. Appl. Phys. 27, 1537 (1956).
8. K. Amokosu and J. Imoi, "Emission Decay Phenomena Due to the Contaminated Anode," J. Appl. Phys. 24, 107 (1953).
9. D. A. Campbell, "Long Pulse Performance of Oxide Coated Cathodes," Ph. D. Thesis, University of Minnesota (September 1962).
10. A. S. Eisenstein, "Some Properties of the  $\text{Ba}_2\text{SiO}_4$  Oxide Cathode Interface," J. Appl. Phys. 20, 776 (1949).
11. W. E. Romsey, "A General Survey of Sparking Phenomena in High Vacuum Thermionic Tubes," NDRC Division 14, Report 516 (31 October 1945).
12. W. E. Donforth and D. L. Goldwater, "Resistance of Oxide Cathode Coatings for High Values of Pulsed Emission," J. Appl. Phys. 20, 163 (1949).
13. R. W. Olthuis, "An Ultraclean Diode as an Emission Tester for Microwave Applications," ASTM Special Publication No. 246 (1958).
14. F. T. Worrell, "Some Tests of Ionization Gages," Technical Report 298, Lincoln Laboratory, M. I. T. (18 February 1963), DDC 402407.
15. R. Dehn, "A New Method for the Measurement of Rapid Fluctuations of Temperature," Brit. J. Appl. Phys. 7, 144 (1956).
16. \_\_\_\_\_, "The Mechanism of Pulse Temperature Rise on the Surface of Thermionic Cathodes," Brit. J. Appl. Phys. 7, 210 (1956).
17. L. N. Vogin, "Temperature State of Oxide Cathodes in Pulse Discharges," Radio Engineering and Electronic Physics (U. S. S. R.) 7, 1500 (1962).
18. Semiannual Technical Summary Report to ARPA on the High-Power Tube Program, Lincoln Laboratory, M. I. T. (30 June 1963), pp. 15-16, DDC 411458.
19. G. E. Vibrons, "Calculation of the Surface Temperature of a Solid under Electron Bombardment," Technical Report 268, Lincoln Laboratory, M. I. T. (16 November 1962), DDC 294645.

20. N. B. Hannay, D. MacNair, and A. H. White, "Semi-Conducting Properties in Oxide Cathodes," *J. Appl. Phys.* 20, 669 (1949).
21. R. Loosjes and H. J. Vink, "Conduction Mechanism in Oxide Coated Cathodes," *Philips Research Reports* 4, 449 (1949).
22. A. M. Clagston, *Microwave Magnetrons*, G. B. Collins, ed., Radiation Laboratory Series, M. I. T. (McGraw-Hill, New York, 1948), Vol. 6, p. 521.
23. E. A. Coomes, "Thermionic Cathodes and Their Vacuum Environment," Discussion Series at Eitel-McCullough, Inc. (September 1955), DDC 78498.
24. C. G. J. Jansen, R. Loosjes, and K. Campoon, "Velocity Distribution of Electrons of Thermionic Emitters Under Pulsed Operation," *Philips Research Reports* 9, 241 (1954).
25. C. M. Lavett, "Some Measurements of the Electrical Conduction of Oxide Cathodes," *Proc. Phys. Soc.* 67B, 387 (1954).



## DOCUMENT CONTROL DATA - R&amp;D

(Security classification of title, body of abstract and indexing annotation must be entered when the overall report is classified)

1. ORIGINATING ACTIVITY (Corporate author)

Lincoln Labs., Lexington, Mass.

2a. REPORT SECURITY CLASSIFICATION

UNCLASSIFIED

2b. GROUP

N/A

3. REPORT TITLE

Limitations of Oxide-Cathode High Current Density Operation

4. DESCRIPTIVE NOTES (Type of report and inclusive dates)

Technical Report

5. AUTHOR(S) (Last name, first name, initial)

Pike, H.A.

6. REPORT DATE

22 May 64

7a. TOTAL NO. OF PAGES

21

7b. NO. OF REFS

25

8a. CONTRACT OR GRANT NO.

AF19(628)500

b. PROJECT NO.

9a. ORIGINATOR'S REPORT NUMBER(S)

TR-356

c.

9b. OTHER REPORT NO(S) (Any other numbers that may be assigned this report)

d.

ESD-TDR-64-332

10. AVAILABILITY/LIMITATION NOTICES

Qualified Requesters May Obtain Copies From DDC.

11. SUPPLEMENTARY NOTES

12. SPONSORING MILITARY ACTIVITY

ESD, L.G. Hanscom Field, Bedford, Mass.

13. ABSTRACT

Microsecond pulsed current from a good oxide cathode at normal operating temperatures is often limited by sparking rather than by saturation of cathode emission. Measurements have been made of the current at which sparking occurs for pulse lengths between 0.5 and 500 usec. Also, the fast time response of photomultiplier tubes sensitive in the near infrared has allowed the measurement of temperature transients on the cathode surface during and after the pulse. It was found that the current which caused a fixed cathode surface temperature rise was dependent upon pulse length, as was the sparking current. The supposition is made that, for short pulses, sparking is associated with the thermal dissociation of the cathode coating surface due to joule heat generated by the passage of current through the high resistance layer at the surface of the coatings. Increasing the anode temperature decreased both the cathode work function and coating resistance. Using this technique, current density in excess of 20 amp/cm<sup>2</sup> was drawn without sparking.



14. KEY WORDS	LINK A		LINK B		LINK C	
	ROLE	WT	ROLE	WT	ROLE	WT
Measurements Temperature Experimental Sparking						

INSTRUCTIONS

1. **ORIGINATING ACTIVITY:** Enter the name and address of the contractor, subcontractor, grantee, Department of Defense activity or other organization (*corporate author*) issuing the report.
- 2a. **REPORT SECURITY CLASSIFICATION:** Enter the overall security classification of the report. Indicate whether "Restricted Data" is included. Marking is to be in accordance with appropriate security regulations.
- 2b. **GROUP:** Automatic downgrading is specified in DoD Directive 5200.10 and Armed Forces Industrial Manual. Enter the group number. Also, when applicable, show that optional markings have been used for Group 3 and Group 4 as authorized.
3. **REPORT TITLE:** Enter the complete report title in all capital letters. Titles in all cases should be unclassified. If a meaningful title cannot be selected without classification, show title classification in all capitals in parenthesis immediately following the title.
4. **DESCRIPTIVE NOTES:** If appropriate, enter the type of report, e.g., interim, progress, summary, annual, or final. Give the inclusive dates when a specific reporting period is covered.
5. **AUTHOR(S):** Enter the name(s) of author(s) as shown on or in the report. Enter last name, first name, middle initial. If military, show rank and branch of service. The name of the principal author is an absolute minimum requirement.
6. **REPORT DATE:** Enter the date of the report as day, month, year, or month, year. If more than one date appears on the report, use date of publication.
- 7a. **TOTAL NUMBER OF PAGES:** The total page count should follow normal pagination procedures, i.e., enter the number of pages containing information.
- 7b. **NUMBER OF REFERENCES:** Enter the total number of references cited in the report.
- 8a. **CONTRACT OR GRANT NUMBER:** If appropriate, enter the applicable number of the contract or grant under which the report was written.
- 8b, 8c, & 8d. **PROJECT NUMBER:** Enter the appropriate military department identification, such as project number, subproject number, system numbers, task number, etc.
- 9a. **ORIGINATOR'S REPORT NUMBER(S):** Enter the official report number by which the document will be identified and controlled by the originating activity. This number must be unique to this report.
- 9b. **OTHER REPORT NUMBER(S):** If the report has been assigned any other report numbers (*either by the originator or by the sponsor*), also enter this number(s).
10. **AVAILABILITY/LIMITATION NOTICES:** Enter any limitations on further dissemination of the report, other than those

imposed by security classification, using standard statements such as:

- (1) "Qualified requesters may obtain copies of this report from DDC."
- (2) "Foreign announcement and dissemination of this report by DDC is not authorized."
- (3) "U. S. Government agencies may obtain copies of this report directly from DDC. Other qualified DDC users shall request through \_\_\_\_\_."
- (4) "U. S. military agencies may obtain copies of this report directly from DDC. Other qualified users shall request through \_\_\_\_\_."
- (5) "All distribution of this report is controlled. Qualified DDC users shall request through \_\_\_\_\_."

If the report has been furnished to the Office of Technical Services, Department of Commerce, for sale to the public, indicate this fact and enter the price, if known.

11. **SUPPLEMENTARY NOTES:** Use for additional explanatory notes.
12. **SPONSORING MILITARY ACTIVITY:** Enter the name of the departmental project office or laboratory sponsoring (*paying for*) the research and development. Include address.
13. **ABSTRACT:** Enter an abstract giving a brief and factual summary of the document indicative of the report, even though it may also appear elsewhere in the body of the technical report. If additional space is required, a continuation sheet shall be attached.

It is highly desirable that the abstract of classified reports be unclassified. Each paragraph of the abstract shall end with an indication of the military security classification of the information in the paragraph, represented as (TS), (S), (C), or (U).

There is no limitation on the length of the abstract. However, the suggested length is from 150 to 225 words.

14. **KEY WORDS:** Key words are technically meaningful terms or short phrases that characterize a report and may be used as index entries for cataloging the report. Key words must be selected so that no security classification is required. Identifiers, such as equipment model designation, trade name, military project code name, geographic location, may be used as key words but will be followed by an indication of technical context. The assignment of links, rules, and weights is optional.